Analysis of Optical Flow Constraints

Alberto Del Bimbo, *Member, IEEE*, Paolo Nesi, *Member, IEEE*, and Jorge L. C. Sanz, *Senior Member, IEEE*

Abstract—Different constraint equations have been proposed in the literature for the derivation of optical flow. Despite of the large number of papers dealing with computational techniques to estimate optical flow, only a few authors have investigated conditions under which these constraints exactly model the velocity field, that is, the perspective projection on the image plane of the true 3-D velocity. In this paper, these conditions are analyzed under different hypotheses, and the departures of the constraint equations in modeling the velocity field are derived for different motion conditions. Experiments are also presented giving measures of these departures and of the induced errors in the estimation of the velocity field.

I. INTRODUCTION

G RADIENT-BASED techniques for the estimation of the projection of the 3-D motion on the image plane [1]–[6], as opposed to spatio-temporal filtering [7]–[10] and correspondence-based approaches [11], [12], are concerned with the observation of brightness changes in the image plane. The flow field of these changes is commonly referred to as "optical flow" or "image flow" [1], [13], [14]. Optical flow was originally defined as the solution of a constraint equation, which is commonly referred to as the optical flow constraint (OFC), and derived under the assumption that image brightness is stationary in every point of the image [1]. A modified constraint equation, which is similar to OFC but includes the divergence of the optical flow, was later proposed in [15]–[17]. This was defined assuming the conservation of the density of image features, provided that their size remains constant in time. However, as argued in [13], the feature density cannot be substituted to the image brightness for a proper analysis. A version of this constraint (modeling image brightness changes instead of feature density changes) was proposed in [6] and referred to as the extended optical flow constraint (EOFC).

Generally speaking, optical flow field as modeled by OFC or EOFC and differs from the perspective projection of the 3-D motion on the image plane, which is commonly referred to as "velocity field," "motion field," or "displacement rate field." Since the velocity field is a purely geometric concept and the optical flow concept is based on the observation of the changes in the image brightness, in many cases, the optical flow only represents an approximation of the velocity field [17], [13].

Two sources of approximation exist. The first is connected to the techniques used for solving the constraint equations. Since the constraint equations define an ill-posed model,

additional constraints are needed to estimate the optical flow field. Therefore, depending on the additional constraints and computational techniques used, many different optical flows can be computed that exhibit different behaviors in different conditions, e.g., [1]–[5], [18]. The second source of approximation depends on the extent to which the constraint equation actually models the velocity field. Conditions under which the velocity field is exactly modeled by OFC were analyzed in [19] and [14] under orthographic and perspective projection, whereas effects due to the absence of calibration of the optical system were expounded in [13]. Considerations about the opportunity of using the modified constraint were briefly exposed in [16], [17], and [13]. Experimental comparisons between estimations of the optical flow based on OFC and EOFC were reported in [20] and [21] by using multipoint computational techniques. A comparative evaluation between OFC and EOFC was also reported in [22]. However, the experiments reported in that paper were not supported by any analytical demonstration, and results presented contrast with the definitions of OFC and EOFC due to the coarse errors produced by the computation of partial derivatives of the image brightness.

In this paper, analytical expressions of the departures of OFC and EOFC constraint equations in modeling the velocity field under different conditions are derived. Effects of these departures on the estimation of the velocity field are also evaluated. The analysis is carried out for both cases of isotropic and uniform illumination, considering effects of calibration and noncalibration of the optical system. Conclusions derived analytically are experimentally validated with synthetic test image sequences.

The paper is organized as follows. In Section II, a short review of basic concepts is reported. In Section III, the conditions for the applicability of OFC and EOFC equations for modeling the velocity field are analyzed. Analytical expressions of the departures of the OFC and EOFC in modeling the velocity field in most relevant cases of motion are derived and discussed in Section IV. Experimental evidence of these results is finally presented in Section V. Conclusions are drawn in Section VI.

II. BASIC NOTIONS

A. The Velocity Field

The velocity field is defined as the perspective projection on the image plane of the real 3-D object velocity [23]. Given a point P in the 3-D space identified by the vector $P = (X, Y, Z)^t$, its perspective projection on the image plane with focal length $Z = 1$ is $p = (x, y, l)^t$, where x, y, l, are
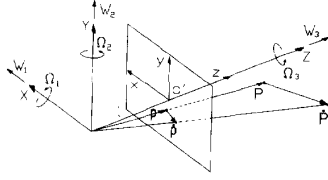
Fig. 1. Reference systems of coordinates and the velocity field vectors defined as the projection on the image plane of the true 3-D velocity.

taken with reference to the system of coordinates centered in o' (see Fig. 1). Therefore, the following relationship holds:

$$\mathbf{p} = \frac{l}{Z}\mathbf{P}. \tag{1}$$

The projection of the 3-D motion on the image plane, which is commonly referred to as "velocity field," is obtained by taking derivatives on (1)

$$\dot{\mathbf{p}} = \frac{l}{Z}\left(\dot{\mathbf{P}} - \mathbf{P}\frac{\dot{\mathbf{P}} \cdot \hat{\mathbf{Z}}}{Z}\right) \tag{2}$$

where $\hat{\mathbf{Z}}$ is the Z-axis unit vector. The 3-D motion of the generic point $\mathbf{P}$ can be modeled as comprised of translational and rotational velocity components

$$\dot{\mathbf{P}} = \mathbf{W} + \boldsymbol{\Omega} \times \mathbf{P} \tag{3}$$

where $\mathbf{W} = (W_1, W_2, W_3)^t$ and $\boldsymbol{\Omega} = (\Omega_1, \Omega_2, \Omega_3)^t$ are the components of the instantaneous translation and rotation, respectively. Substituting (1) and (3) in (2), two scalar equations are obtained which express relationships between the components $\dot{p}_1, \dot{p}_2$ of velocity field $\dot{\mathbf{p}}$ and the 3-D motion components of point $\dot{\mathbf{P}}$

$$\dot{p}_1 = \frac{lW_1}{Z} - x\frac{W_3}{Z} + l\Omega_2 - y\Omega_3 - x\frac{y\Omega_1 - x\Omega_2}{l}, \tag{4}$$

$$\dot{p}_2 = \frac{lW_2}{Z} - y\frac{W_3}{Z} + x\Omega_3 - l\Omega_1 - y\frac{y\Omega_1 - x\Omega_2}{l}. \tag{5}$$

B. The Image Brightness

The image brightness can be considered as the measure of the irradiance of the scene on the image plane. According to the geometric relationships shown in Fig. 2 and the above notation, its expression under perspective projection is

$$E(x(t), y(t), t) =$$

$$L(\rho(\mathbf{p}, t), \mathbf{N}_s(\mathbf{P}), \mathbf{N}_e(\mathbf{P}))\frac{\pi}{4}\left(\frac{D}{l}\right)^2\frac{\left(\mathbf{P} \cdot \hat{\mathbf{Z}}\right)^4}{(\mathbf{P} \cdot \mathbf{P})^2} \tag{6}$$

where $L(\rho(\mathbf{p}, t), \mathbf{N}_s(\mathbf{P}), \mathbf{N}_e(\mathbf{P}))$ is the radiance of the scene; $\rho(\mathbf{p}, t)$ is the albedo that describes the spatial variations of the painted surface texture of the scene under observation; t is the time; $N_e(\mathbf{P})$ is the unit vector that identifies the direction of light source; $N_s(\mathbf{P})$ is the unit vector normal to the scene surface; D is the diameter of the lens; and the last term is the fourth power of the angle α between the vector $\mathbf{P}$ and the Z axis [24].
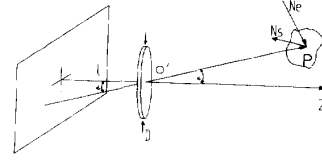

Fig. 2. Geometry of the optical system.

As pointed out by Horn in [25], the radiance can be regarded as the product

$$L(\rho(\mathbf{p}, t), \mathbf{N}_s(\mathbf{P}), \mathbf{N}_e(\mathbf{P})) = \rho(\mathbf{p}, t) \ R(\mathbf{N}_s(\mathbf{P}), \mathbf{N}_e(\mathbf{P})) \tag{7}$$

of the albedo $\rho(\mathbf{p}, t)$ and the reflectance $R(\mathbf{N}_s(\mathbf{P}), \mathbf{N}_e(\mathbf{P}))$, which takes into account the variations of radiance due to changes in the surface orientation with respect to the direction of the light source illumination. Both these terms are functions of the 3-D spatial coordinates of $\mathbf{P}$.

The optical system can be calibrated considering its geometry [25]. In this case, the irradiance can be considered to be equal to the radiance

$$E(x(t), y(t), t) = L(\rho(\mathbf{p}, t), \mathbf{N}_s(\mathbf{P}), \mathbf{N}_e(\mathbf{P})). \tag{8}$$

From the point of view of dimensionality, the radiance $L()$ is the power per unit area per unit solid angle emitted by the scene surface in a given direction, and the image brightness E is the ratio between the power received by an image element and the element size. Therefore, the image brightness is not a point property but an energy density commonly expressed in watts per meter squared [26].

III. OPTICAL FLOW CONSTRAINT EQUATIONS

In this section, the two different constraints proposed in the literature to derive the optical flow are analyzed, considering conditions under which these exactly model the velocity field.

A. The Optical Flow Constraint

Originally, the optical flow has been defined as the solution of a constraint equation: the optical flow constraint (OFC) [1]. It has been derived under the assumption that the image brightness in each image point is stationary with respect to t (i.e., $dE/dt = 0$)

$$\frac{dE}{dt} = \frac{\partial E}{\partial x}\frac{dx}{dt} + \frac{\partial E}{\partial y}\frac{dy}{dt} + \frac{\partial E}{\partial t} = 0. \tag{9}$$

This equation can also be rewritten as

$$E_x v_1 + E_y v_2 + E_t = 0 \tag{10}$$

where the abbreviation for partial derivatives of the image brightness has been introduced, and v_1, v_2 correspond to dx/dt, dy/dt and represent the components of the *local velocity vector* $\mathbf{v}$ (i.e., the optical flow) along the x and y directions, respectively. According to the notation introduced, (9) can be rewritten as

$$\nabla E(\mathbf{p}, t) \cdot \mathbf{v} + E_t(\mathbf{p}, t) = 0. \tag{11}$$

The OFC equation alone does not provide enough constraints to determine the optical flow components (it is an ill-posed problem [1], [27], [18]). In fact, it can be directly used only to estimate the optical flow component parallel to the image brightness gradient $\nabla E(\mathbf{p}, t)$ [14]

$$\mathbf{v}_\perp = -\frac{E_t}{\|\nabla E\|} \frac{\nabla E}{\|\nabla E\|} \tag{12}$$

where $E = E(\mathbf{p}, t)$, and $\frac{\nabla E}{\|\nabla E\|}$ is the unit vector identifying the direction of ∇E if $\nabla E \neq 0$, and $dE/dt = 0$. The indeterminacy in estimating the optical flow can be considered an instance of the well-known *problem of aperture* [1].

1) Considerations About the OFC: The relationships between the optical flow as modeled by the OFC and the velocity field were analyzed and discussed by several authors.

Schunck pointed out simplifications about scene surfaces and illumination that justify the OFC equation from the physics point of view but without giving any analytical evidence. Specifically, under *orthographic projection*, in [1], [15], [28], he required that i) the perceived change in image irradiance at each point in the image plane is entirely due to translational motion, and ii) the image must be smooth except at a finite number of boundary discontinuities.

It was later clarified that the applicability of the OFC is ensured if the changes in image irradiance in each point of the image are only due to the motion of image pattern and not to the changes in pattern due to reflectance effects (i.e., deformations due to changes in direction of the illumination source and changes in direction of the normal of the surface) [19], [17]. Such a condition is satisfied by "*the image of a translating, diffuse object with distant light sources*" [29], where "*diffuse*" should be synonymous with Lambertian surfaces (e.g., the surfaces irradiate the received radiation in outward directions), and "*distant light sources*" should be an approximation of uniform illumination (the direction of illumination is the same in all points, which can be approximated by having a point-source of light very far from the scene).

A more formal analysis was developed by Verri and Poggio in [14]. They found that under *perspective projection*, if the object motion is translational (with a calibrated optical system, uniform illumination, and scene objects with Lambertian surfaces), then the component of velocity field parallel to the ∇E is equal to the optical flow as derived from the OFC. They also analyzed the case of nonuniform illumination with translational and rotational motion, observing that in these cases, the velocity field is not equal to optical flow.

In [13], Nagel demonstrated that under *perspective projection* with isotropic constant illumination, Lambertian surfaces, and a noncalibrated optical system, if the displacement field (i.e., the velocity field) is substituted in the OFC equation, then $dE/dt \neq 0$. This shows that the OFC does not exactly model the velocity field. The term that makes $dE/dt \neq 0$ takes into account geometric and radiometric effects mainly due to *noncalibration* of the optical system.

A common assumption for ensuring the applicability of the OFC is that the moving object must be covered by a significative pattern. Otherwise, since, in that case, E_x and E_y are equal to zero, the optical flow cannot be estimated [1], [19],

TABLE I
SUMMARY OF THE MOTION CONDITIONS THAT GUARANTEE THE EQUALITY BETWEEN THE OPTICAL FLOW (AS DEFINED BY THE OFC) AND THE VELOCITY FIELD (i.e., $\mathbf{v}_\perp = \mathbf{p}_\perp$) UNDER CONDITIONS OF LAMBERTIAN SURFACES, LOCALLY RIGID PATTERN, AND CONSTANT ILLUMINATION

Type of projection	Isotropic illumination	Uniform illumination
orthographic	all	only translational
perspective without calibration	only rotational around Z-axis	none
perspective with calibration	all	only translational

[25]. E_x and E_y could be different from zero in the presence of perspective projection and/or nonisotropic light sources. In fact, in these situations, changes in image brightness can be due only to reflectance effects instead of object motion.

These results are resumed and completed in the rest of this section for isotropic and uniform illuminations and calibrated and noncalibrated optical systems. It is assumed that the radiance is independent of surface orientation—i.e., that objects have Lambertian surfaces. Conclusions are summarized in Table I.

2) Isotropic Light Source: a) In the case of *perspective projection, if the optical system is calibrated*, then the image brightness takes the form

$$E(\mathbf{p}, t) = L(\rho(\mathbf{p}, t)) = \rho(\mathbf{p}, t)$$

and the total derivative of the image brightness $E = E(\mathbf{p}, t)$ with respect to t is expressed by

$$\frac{dE}{dt} = \nabla \rho(\mathbf{p}, t) \cdot \dot{\mathbf{p}} + \rho_t(\mathbf{p}, t). \tag{13}$$

If the patterns on the moving objects in the scene are supposed to be locally rigid (i.e., $d\rho(\mathbf{p}, t)/dt = 0$), (13) modeling the velocity field assumes the form

$$\nabla \rho(\mathbf{p}, t) \cdot \dot{\mathbf{p}} + \rho_t(\mathbf{p}, t) = 0 \tag{14}$$

which is structurally equal to the OFC.

Therefore, in the case of isotropic light source, the OFC is an appropriate model for the velocity field without imposing any restrictions on object motion.

b) In the case of *perspective projection, if the optical system is noncalibrated*, then (6) is rewritten as

$$E(\mathbf{p}, t) = \rho(\mathbf{p}, t) \frac{\pi}{4} \left(\frac{D}{l} \right)^2 \frac{(\mathbf{P} \cdot \hat{\mathbf{Z}})^4}{(\mathbf{P} \cdot \mathbf{P})^2}. \tag{15}$$

In these conditions, the OFC does not model the velocity field. In fact, the total derivative of the irradiance with respect to t (see Appendix A) assumes the form

$$\frac{dE}{dt} = (\nabla \rho(\mathbf{p}, t) \cdot \dot{\mathbf{p}} + \rho_t(\mathbf{p}, t)) \frac{\pi}{4} \left(\frac{D}{l} \right)^2 \frac{(\mathbf{P} \cdot \hat{\mathbf{Z}})^4}{(\mathbf{P} \cdot \mathbf{P})^2}$$
$$+ 4E \left(\frac{\dot{\mathbf{P}} \cdot \hat{\mathbf{Z}}}{Z} - \frac{\mathbf{P} \cdot \dot{\mathbf{P}}}{\mathbf{P} \cdot \mathbf{P}} \right). \tag{16}$$

The first term on the right side vanishes if the pattern on the moving objects in the scene is supposed to be locally rigid. In this case, (16) becomes

$$\frac{dE}{dt} = 4E \left(\frac{\dot{\mathbf{P}} \cdot \hat{\mathbf{Z}}}{Z} - \frac{\mathbf{P} \cdot \dot{\mathbf{P}}}{\mathbf{P} \cdot \mathbf{P}} \right) \tag{17}$$

which is the same expression as the one obtained by Nagel in [13] following a different derivation. It should be noted that typically, $\mathbf{P}$, Z, and $\dot{\mathbf{P}}$ are not available, and thus, (17) cannot be used for estimating the velocity field. The right side of (17) is only due to the noncalibration of the optical system and takes into account the perspective projection geometry as well as radiometric aspects.

By using (3), (17) can be rewritten as

$$\frac{dE}{dt} = 4E\left(\frac{\mathbf{W} \cdot \hat{\mathbf{Z}}}{Z} + \frac{\mathbf{\Omega} \times \mathbf{P} \cdot \hat{\mathbf{Z}}}{Z} - \frac{\mathbf{P} \cdot \mathbf{W}}{\mathbf{P} \cdot \mathbf{P}} - \frac{\mathbf{P} \cdot \mathbf{\Omega} \times \mathbf{P}}{\mathbf{P} \cdot \mathbf{P}}\right).$$
(18)

The third term on the right side is due to the cosine of the angle between the vector $\mathbf{P}$ and the vector of the instantaneous translational motion $\mathbf{W}$ (see Fig. 1). If these two vectors form a right angle, this term will be zero, and (18) will reduce to a simpler expression.

Simplifying and expanding the motion components (3), the following expression for dE/dt is obtained

$$\frac{dE}{dt} = 4E\left(\frac{W_3}{Z} + \frac{Y\Omega_1}{Z} - \frac{X\Omega_2}{Z} - \frac{W_1 X + W_2 Y + W_3 Z}{X^2 + Y^2 + Z^2}\right).$$
(19)

From this expression, it can be seen that in the absence of calibration, the OFC can be used properly to model the velocity field due to rotational motions around the Z-axis ($\Omega_3 \neq 0$). In fact, in this case being $W_1 = 0$, $W_2 = 0$, $W_3 = 0$, $\Omega_1 = 0$, and $\Omega_1 = 0$, the result is $dE/dt = 0$.

Equation (19) can also be approximated by the OFC equation when the following occur:

i) The optical system has a very small aperture, and the moving objects in the scene are very far from the center of the reference coordinate system. In this case, the effect due to the lack of calibration can be neglected, and the right side of (19) reduces to zero.

ii) X and Y are close to zero (the points of the moving objects are close to the Z-axis). In this case, the fourth term in (19) reduces to $-W_3/Z$, and thus, the right side of (19) equals zero.

c) If the system is under *orthographic projection* and the moving object has a superimposed locally rigid pattern, then (14) also holds. Therefore, under these conditions, the velocity field is equal to the optical flow as derived from the OFC.

3) *Uniform Light Source:* a) In the case of *perspective projection, if the optical system is calibrated*, then the image brightness assumes the form (8) with the radiance expressed by (7) and the reflectance equal to $\mathbf{N}_s(\mathbf{P}) \cdot \mathbf{N}_e$, and hence

$$E(\mathbf{p}, t) = L(\rho(\mathbf{p}, t), \mathbf{N}_s(\mathbf{P}), \mathbf{N}_e) = \rho(\mathbf{p}, t)\mathbf{N}_s(\mathbf{P}) \cdot \mathbf{N}_e.$$
(20)

Taking the total derivative of the above expression, we have

$$\frac{dE}{dt} = (\mathbf{N}_s(\mathbf{P}) \cdot \mathbf{N}_e)(\nabla\rho(\mathbf{p}, t) \cdot \dot{\mathbf{p}} + \rho_t(\mathbf{p}, t))$$
$$+ \rho(\mathbf{p}, t)(\mathbf{N}_e \cdot \mathbf{\Omega} \times \mathbf{N}_s(\mathbf{P})).$$
(21)

If the motion is only translational, and the patterns on the moving objects in the scene are supposed to be locally rigid

(i.e., $\frac{d\rho(\mathbf{p}, t)}{dt} = 0$), the terms on the right side of (21) are both equal to zero, and thus, $dE/dt = 0$. Since (21) is structurally equal to the OFC, this demonstrates that the OFC can be used properly for modeling the velocity field also under perspective projection, provided that the optical system is calibrated. In addition to what is stated in [14], it is also requested that the patterns in the scene are locally rigid.

b) In the case of *perspective projection, if the optical system is noncalibrated*, then the image brightness assumes the form

$$E(\mathbf{p}, t) = \rho(\mathbf{p}, t)(\mathbf{N}_s(\mathbf{P}) \cdot \mathbf{N}_e)\frac{\pi}{4}\left(\frac{D}{l}\right)^2 \frac{(\mathbf{P} \cdot \hat{\mathbf{Z}})^4}{(\mathbf{P} \cdot \mathbf{P})^2}$$
(22)

and its total derivative is (see Appendix B)

$$\frac{dE}{dt} = 4E\left(\frac{\dot{\mathbf{P}} \cdot \hat{\mathbf{Z}}}{Z} - \frac{\mathbf{P} \cdot \dot{\mathbf{P}}}{\mathbf{P} \cdot \mathbf{P}}\right) + \rho(\mathbf{p}, t)\frac{\pi}{4}\left(\frac{D}{l}\right)^2 \frac{(\mathbf{P} \cdot \hat{\mathbf{Z}})^4}{(\mathbf{P} \cdot \mathbf{P})^2}$$
$$(\mathbf{N}_e \cdot \mathbf{\Omega} \times \mathbf{N}_s(\mathbf{P})).$$
(23)

The structure of (23) differs from (17) only by the presence of the last term. The term $\mathbf{N}_e \cdot \mathbf{\Omega} \times \mathbf{N}_s(\mathbf{P})$ of (23) vanishes when the following hold:

i) The motion is translational (i.e., $\mathbf{\Omega} = 0$).

ii) The unit vector normal to the scene surface $\mathbf{N}_s(\mathbf{P})$ is parallel to $\mathbf{\Omega}$ or $\mathbf{N}_e$.

iii) $\mathbf{\Omega}$ is parallel to the direction of light source $\mathbf{N}_e$.

Under any of these conditions, (17) and (23) are structurally equal. Therefore, there do not exist any motion conditions in which dE/dt (in the form of (23)) is equal to zero. In this case, the optical flow is always different from the velocity field.

c) If the system is under *orthographic projection* and the moving object has a superimposed locally rigid pattern, then the OFC properly models the velocity field, as pointed out in [1] and [15].

B. The Extended Optical Flow Constraint

As noted by Schunck, the OFC is very similar to the continuity equation of fluid dynamics that derives from the law of conservation of the mass for incompressible fluids [30]. Based on this fact and observing that the premises on which OFC holds are very restrictive to be met in practice, in [15], Schunck proposed a modified optical flow constraint equation. From the structural point of view, this constraint equation was similar to the OFC except that it was derived for *image feature density* N and included an additional term containing the divergence of the optical flow

$$\nabla \cdot (N\mathbf{d}) + \frac{\partial N}{\partial t} = 0$$
(24)

where

$$\nabla \cdot (N\mathbf{d}) = \mathbf{d} \cdot \nabla N + N\nabla \cdot \mathbf{d}.$$
(25)

Equation (24) defines an alternative "optical flow," $\mathbf{d}$, which in general is different from the one obtained by the OFC equation. Equation (24) can be rewritten as

$$N_x d_1 + N_y d_2 + N d_{1x} + N d_{2y} + N_t = 0$$
(26)

where (d_1, d_2) are the optical flow components of $\mathbf{d}$ on the image plane.

Schunck, in [15]–[17], affirmed that this modified constraint equation would be a better model than the OFC in the presence of perspective projection especially for rotational motions if the light source is isotropic and the scene surfaces are Lambertian. A formal derivation for the modified constraint equation was presented by Schunck in [16] and [17]. This derivation was based on the conservation of the *density of the image brightness features* N, assuming that the size of the features remains constant with respect to time (no deformation due to motion and/or reflectance exists). He noticed that the modified constraint equation can be applied to the image brightness E instead of N only when the illumination is isotropic. In fact, in this condition, the image brightness behaves like a density, and the OFC cannot be used.

Arguments supporting this theory were developed by Nagel in [13], who argued that features are themselves entities derived from spatial variations of image brightness and cannot be substituted for a proper analysis of image brightness. The image brightness is the limit for the vanishing of the ratio between the power received by an image plane element and the size of this element [24], [25] (i.e., it is an energy density usually expressed in Watts per meter squared). Based on these considerations, in [6], a new constraint equation, called the extended optical flow constraint (EOFC), was introduced

$$E_x d_1 + E_y d_2 + E d_{1x} + E d_{2y} + E_t = 0 \qquad (27)$$

where d_1 and d_2 are the components of the optical flow vector **d**. From the point of view of the constraint structure, the EOFC (27) differs from the OFC (10) only by the term involving the divergence of the optical flow field vector $(E\nabla \cdot \mathbf{d})$ and differs from (26) because the EOFC models the changes in image brightness E, instead of image feature density N.

OFC and EOFC have been compared by using the same computational techniques in [20] and [21]. Performances with respect to other selected OFC-based computational techniques were also reported. EOFC has proved to be superior to the OFC in certain motion conditions in the absence of calibration.

IV. MODELING VELOCITY FIELD BY OFC AND EOFC

The optical flow fields derived from (11) and (27) do not model exactly the velocity field except in special conditions as discussed in the previous sections. Generally speaking, substituting $\dot{\mathbf{p}}$ for **v** in (11) and (27), we have

$$\nabla E \cdot \dot{\mathbf{p}} + E_t = \mathcal{E}_{\text{ofc}}, \qquad (28)$$

$$\nabla E \cdot \dot{\mathbf{p}} + E\nabla \cdot \dot{\mathbf{p}} + E_t = \mathcal{E}_{\text{eofc}} \qquad (29)$$

where $\mathcal{E}_{\text{ofc}}$ and $\mathcal{E}_{\text{eofc}}$ are the departures of the OFC and EOFC equations in modeling the velocity field, respectively, and depend on $\mathbf{p}$, $\dot{\mathbf{P}}$ and E. By taking the difference between (28) and (10) and between (29) and (27), the following expressions are obtained:

$$\nabla E \cdot (\dot{\mathbf{p}} - \mathbf{v}) = \mathcal{E}_{\text{ofc}}, \qquad (30)$$

$$\nabla E \cdot (\dot{\mathbf{p}} - \mathbf{d}) + E\nabla \cdot (\dot{\mathbf{p}} - \mathbf{d}) = \mathcal{E}_{\text{eofc}} \qquad (31)$$

from which errors in estimating the velocity field can be derived for the cases of OFC and EOFC as a function of the departures.

For the OFC, developing the scalar product of (30), the error in estimating the velocity field is given

$$\eta_{\text{ofc}} = \|(\dot{\mathbf{p}} - \mathbf{v})\| = \frac{\mathcal{E}_{\text{ofc}}}{\|\nabla E\| \cos(\theta)} \qquad (32)$$

where θ is the angle between ∇E and the difference between the correct velocity field and the estimated optical flow. From the above equation, it can be noted that η_{ofc} vanishes with $\mathcal{E}_{\text{ofc}}$ or if ∇E is very large. Since η_{ofc} depends on the angle θ, only the component of η_{ofc}, which is parallel to the ∇E, can be directly estimated (for $\cos(\theta) = 1$, if $\|\nabla E\| \neq 0$)

$$\eta_{\text{ofc}\perp} = \frac{\mathcal{E}_{\text{ofc}}}{\|\nabla E\|} \frac{\nabla E}{\|\nabla E\|}. \qquad (33)$$

Therefore, if the value of the departure from the model $\mathcal{E}_{\text{ofc}}$ is known, then the error $\eta_{\text{ofc}\perp}$ can be estimated. It should be noted that $\eta_{\text{ofc}\perp}$ equal to zero (with $\nabla E \neq 0$ and $\cos(\theta) \neq 0$) does not guarantee that the velocity field $\dot{\mathbf{p}}$ and the optical flow **v** are equal but only that their components parallel to ∇E are (e.g., $\dot{\mathbf{p}}_\perp = \mathbf{v}_\perp$).

For the EOFC, (31) is a partial differential equation describing an ill-posed problem that cannot be solved directly in order to obtain the field $(\dot{\mathbf{p}} - \mathbf{d})$. An approximation of the error in the estimation of the optical flow along the direction of ∇E can be obtained by following the same derivation as above. Thus

$$\eta_{\text{eofc}\perp} = \frac{\mathcal{E}_{\text{eofc}}}{\|\nabla E\|} \frac{\nabla E}{\|\nabla E\|} \qquad (34)$$

where the term $\frac{E\nabla \cdot (\dot{\mathbf{p}} - \mathbf{d})}{\|\nabla E\|}$ has been neglected with respect to $\frac{\mathcal{E}_{\text{eofc}}}{\|\nabla E\|}$.

For the sake of simplicity, in the following, we will refer to the conditions $\eta_{\text{ofc}\perp} = 0$ or $\eta_{\text{eofc}\perp} = 0$ when the optical flow is said to be equal to the velocity field.

In the rest of this section, analytical expressions for the departures of the OFC and EOFC in modeling the velocity field ($\mathcal{E}_{\text{ofc}}$ and $\mathcal{E}_{\text{eofc}}$) in the presence of different motion conditions are derived and discussed for the two cases of isotropic and uniform light sources. The derivations are based on the assumptions of Lambertian surfaces and noncalibrated optical system.

A. Isotropic Light Source

If the scene patterns are locally rigid, then expression (19) is the exact analytical formulation of dE/dt. Let $\dot{\mathbf{p}} = (\dot{p}_1, \dot{p}_2)$ be a velocity field vector for the image sequence; then, the following two expressions

$$\mathcal{E}_{\text{ofc}} = E_x \dot{p}_1 + E_y \dot{p}_2 + E_t$$
$$= 4E\left(\frac{W_3}{Z} + \frac{Y\Omega_1}{Z} - \frac{X\Omega_2}{Z} - \frac{W_1 X + W_2 Y + W_3 Z}{X^2 + Y^2 + Z^2}\right) \qquad (35)$$

and

$$\mathcal{E}_{\text{eofc}} = E_x \dot{p}_1 + E_y \dot{p}_2 + E\dot{p}_{1x} + E\dot{p}_{2y} + E_t \qquad (36)$$

define a measure of the departure of the OFC and the EOFC equations, respectively, when these are used to estimate the velocity field ($\dot{p}_1$, $\dot{p}_2$).

By using (4) and (5), the following relationship holds:

$$\nabla \cdot \dot{\mathbf{p}} = \dot{p}_{1x} + \dot{p}_{2y} = -2\frac{W_3}{Z} - 3\frac{y\Omega_1}{l} + 3\frac{x\Omega_2}{l} \qquad (37)$$

and the analytical expression of the departure $\mathcal{E}_{\text{eofc}}$ can be directly derived from (36), (37), and (35)

$$\mathcal{E}_{\text{eofc}} = E\left(2\frac{W_3}{Z} + \frac{Y\Omega_1}{Z} - \frac{X\Omega_2}{Z}\right.$$
$$\left. -4\frac{W_1X + W_2Y + W_3Z}{X^2 + Y^2 + Z^2}\right). \qquad (38)$$

Therefore, the following conclusions can be derived regarding the departures of OFC and EOFC in modeling the velocity field.

1) Rotation Around the Z-Axis: In the case of pure rotation around the Z-axis (i.e., $W_1 = 0$, $W_2 = 0$, $W_3 = 0$, $\Omega_1 = 0$, $\Omega_2 = 0$) the term on the right side of (19) is null. Therefore, the departures of the OFC and EOFC in modeling the velocity field are both equal to zero

$$\mathcal{E}_{\text{ofc}} = \mathcal{E}_{\text{eofc}} = 0.$$

2) Translation Parallel to the Image Plane: In the case of translational motion parallel to the image plane (i.e., $W_3 = 0$, $\Omega_1 = 0$, $\Omega_2 = 0$), the departures of the OFC (35) and EOFC (38) in modeling the velocity field are both equal to

$$\mathcal{E}_{\text{ofc}} = \mathcal{E}_{\text{eofc}} = 4E\left(-\frac{W_1X + W_2Y}{X^2 + Y^2 + Z^2}\right). \qquad (39)$$

In the case in which W_1X and W_2Y are equal in module but different in sign, both $\mathcal{E}_{\text{ofc}}$ and $\mathcal{E}_{\text{eofc}}$ vanish.

3) Expansion or Contraction: In the case of pure expansion or contraction (i.e., $W_1 = 0$, $W_2 = 0$, $\Omega_1 = 0$, $\Omega_2 = 0$), the departures of the OFC (35) and EOFC (38) in modeling the velocity field are, respectively

$$\mathcal{E}_{\text{ofc}} = E\left(\frac{4W_3}{Z} - \frac{4W_3Z}{X^2 + Y^2 + Z^2}\right),$$
$$\mathcal{E}_{\text{eofc}} = E\left(\frac{2W_3}{Z} - \frac{4W_3Z}{X^2 + Y^2 + Z^2}\right)$$

due to the optical system geometry since Z is always greater than zero. The above expressions can be rewritten as

$$\mathcal{E}_{\text{ofc}} = 4E\frac{W_3}{Z}(1 - \beta).$$
$$\mathcal{E}_{\text{eofc}} = 4E\frac{W_3}{Z}\left(\frac{1}{2} - \beta\right)$$

where $\beta = Z^2/(X^2 + Y^2 + Z^2)$, and hence, the following relationships hold:

$$|\mathcal{E}_{\text{ofc}}| > |\mathcal{E}_{\text{eofc}}| \quad \text{if} \quad 0 < \beta < 3/4,$$
$$|\mathcal{E}_{\text{ofc}}| = |\mathcal{E}_{\text{eofc}}| \quad \text{if} \quad \beta = 3/4,$$
$$|\mathcal{E}_{\text{ofc}}| < |\mathcal{E}_{\text{eofc}}| \quad \text{if} \quad 3/4 < \beta \leq 1.$$

Considering the perspective projection law (1), the expression $\beta = Z^2/(X^2 + Y^2 + Z^2)$ defines the surface of a sphere in the 3-D space, which projects on the image plane the circle

$$x^2 + y^2 = l^2\frac{(1 - \beta)}{\beta}.$$

For $\beta = 3/4$, we have the circle $x^2 + y^2 = \frac{l^2}{3}$. Hence, to estimate the velocity field, the OFC is a better model than the EOFC for the points that are close to the center of the image, whereas for the points that are farther than $l/\sqrt{3}$ from the center, the EOFC is a more accurate model

$$\text{if } \sqrt{x^2 + y^2} > \frac{l}{\sqrt{3}} \quad \text{then} \quad |\mathcal{E}_{\text{ofc}}| > |\mathcal{E}_{\text{eofc}}|$$

$$\text{if } \sqrt{x^2 + y^2} = \frac{l}{\sqrt{3}} \quad \text{then} \quad |\mathcal{E}_{\text{ofc}}| = |\mathcal{E}_{\text{eofc}}|$$

$$\text{if } \sqrt{x^2 + y^2} < \frac{l}{\sqrt{3}} \quad \text{then} \quad |\mathcal{E}_{\text{ofc}}| < |\mathcal{E}_{\text{eofc}}|.$$

It should be noted that the limit on the image plane depends only on the optical system geometry.

4) Rotation Around X- and Y-Axes: In the case of composite rotation around X- and Y-axes (i.e., $W_1 = 0$, $W_2 = 0$, $W_3 = 0$), the following expressions for the departures of the OFC and EOFC in modeling the velocity field are obtained:

$$\mathcal{E}_{\text{ofc}} = 4E\left(\frac{Y\Omega_1}{Z} - \frac{X\Omega_2}{Z}\right), \quad \mathcal{E}_{\text{eofc}} = E\left(\frac{Y\Omega_1}{Z} - \frac{X\Omega_2}{Z}\right)$$

which lead to the following relationship showing that the EOFC provides a better estimation than the OFC according to a multiplicative factor equal to 4

$$|\mathcal{E}_{\text{ofc}}| = 4|\mathcal{E}_{\text{eofc}}|.$$

Remarks: According to the above discussion, it can be observed that the departure of the EOFC in modeling the velocity field is in most cases less or equal to the departure of the OFC. In particular, the EOFC is verified to be a more appropriate model in the presence of motion along the Z-axis (where $\sqrt{x^2 + y^2} > \frac{l}{\sqrt{3}}$) and rotations around the X- and Y-axes. Moreover, to some extent, the above relationships demonstrate that the EOFC model compensates the effects that are due to the noncalibration of the optical system.

B. Uniform Light Source

If the condition of "isotropic light source" is substituted with the condition of "uniform light source," the total derivative of the image brightness assumes the form expressed by (23). The structure of (23) differs from (17) only by the presence of the last term. Since this term is present in both $\mathcal{E}_{\text{ofc}}$ and $\mathcal{E}_{\text{eofc}}$, the relationships between the departures of the OFC and EOFC models are equal to those presented for the case of isotropic light source.

V. EXPERIMENTAL RESULTS

Relationships between the departures of the OFC and EOFC in modeling the velocity field have been tested by using image
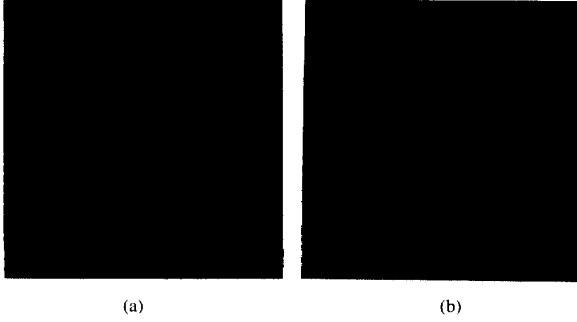
(a)   (b)

Fig. 3. Synthetic sphere under (a) isotropic and (b) uniform illumination (50.0 × 50.0 units).

sequences generated in a controlled environment. The synthetic sequences have been created considering the perspective projection, the camera geometry, the reflectance characteristics, and the conditions of illumination. A high resolution on pixel gray values (32 bits) has been used to approximate a continuous image brightness model and thus reduce the errors introduced in the computing of partial derivatives. It was experimentally found that computational errors by using 8 bits of resolution are larger than those originated by the departures of the OFC and EOFC in modeling the velocity field.

The test sequences consist in the projection of a continuously patterned sphere on a discrete image plane of 128 × 128 pixels corresponding to 50.0 × 50.0 spatial units (see Fig. 3). The sphere is moved in the 3-D space according to different motion conditions. In the reported experiments, the focal length l is equal to 50 units, the dimension of the lens D is equal to 75 units, the radius R of the sphere is equal to 40 units, and the sphere is placed at the first time instant ($t = 0$), in $P = (0, 0, 100)$. According to the perspective projection, the sphere appears on the image plane as a circle with a radius of 20 units ($lX/Z = 50 \cdot 40/100$). The albedo of the sphere consists in a plaid pattern with a period equal to $25/(2\pi R)$ and an amplitude equal to 22 gray level units around the basic value of 90 unit. The surface of the sphere is Lambertian.

The estimates of the departures of the OFC and EOFC models are presented for the cases of isotropic and uniform light sources. For the cases of uniform light source, N_c is taken equal to $(0, 0, 1)$. Types of motions analyzed are as follows:

- translational motion parallel to the image plane: $W = (0.4, -0.4, 0)$ and $\Omega = 0$
- rotational motion around the Z-axis—i.e., parallel to the image plane—$W = 0$ and $\Omega = (0, 0, 0.03)$
- rototranslational motion parallel to the image plane: $W = (0.2, -0.2, 0)$ and $\Omega = (0, 0, 0.015)$
- expansion motion (translational along the Z-axis): $W = (0, 0, 1.1)$ and $\Omega = 0$
- rotational motion in the 3-D space: $W = (0, 0, 0)$ and $\Omega = (0.005, -0.005, 0)$.

The departures of the OFC and EOFC models have been estimated by using the following discrete equations: f

TABLE II
DEPARTURES OF OFC AND EOFC IN MODELING THE
VELOCITY FIELD (MEAN VALUES AND VARIANCES)
(ISOTROPIC ILLUMINATION, NONCALIBRATED OPTICAL SYSTEM)

isotropic illumination - non-calibrated optical system				
Motion	$\hat{\mathcal{E}}_{ofc}$	$\hat{\mathcal{E}}_{eofc}$	$Var(\mathcal{E}_{ofc})$	$Var(\mathcal{E}_{eofc})$
Translational ($W_3 = 0$)	0.401	0.401	0.062	0.062
Rotational around Z-axis	0.035	0.035	0.002	0.002
Parallel to the image plane	0.202	0.202	0.014	0.014
Expansion	0.336	2.288	0.026	0.266
Rotational around X- and Y-axes	0.354	0.096	0.050	0.007

$$\hat{\mathcal{E}}_{ofc}(x, y, t) = E_x(x, y, t)\dot{p}_1(x, y, t)$$
$$+ E_y(x, y, t)\dot{p}_2(x, y, t) + E_t(x, y, t),$$
$$\hat{\mathcal{E}}_{eofc}(x, y, t) = E_x(x, y, t)\dot{p}_1(x, y, t)$$
$$+ E_y(x, y, t)\dot{p}_2(x, y, t)$$
$$+ E(x, y, t)\dot{p}_{1x}(x, y, t)$$
$$+ E(x, y, t)\dot{p}_{2y}(x, y, t) + E_t(x, y, t)$$

where partial derivatives of the image brightness are computed by using central differences (e.g., $E_x(x, y, t) = (E(x + 1, y, t) - E(x - 1, y, t))/2$). The components of velocity field and their derivatives are estimated by means of (4) and (5) on the basis of the 3-D motion components, which are known from the generation of the test sequences.

A. Isotropic Light Source

In Table II, the mean values of the departures of the OFC and EOFC in modeling the velocity field are reported in the case of Lambertian surfaces with a noncalibrated optical system. Mean values of the departures are estimated disregarding the boundaries of the sphere where wide errors are present due to discontinuities (i.e., $\hat{\mathcal{E}} = 1/M \sum_i^M |\hat{\mathcal{E}}|$, where M defines the area of projection of the sphere without boundaries). Results obtained in the first three motion conditions agree with the conclusions derived in Section IV.

In the case of pure expansion, results also agree with the considerations derived in Section IV. In this case, the departures of the OFC and EOFC models depend on the distance from the focus of expansion. In this test sequence, the focus of expansion was set in the center of the coordinate system (the center of the image plane) and $l/\sqrt{3} = 28.8$ units was used (the sphere appears on the image as a circle with a radius of 20 units). Tests have been carried out for different values of focal length l. Results for $l = 10$ (i.e., $l/\sqrt{3} = 5.78$) are reported in Fig. 4 as a function of the distance from the center of the image. In this case, the EOFC produces better results then the OFC only in those points farther than $l/\sqrt{3}$. The dotted area marks regions where discontinuities are present, and therefore, traces in this area do not represent the phenomena under discussion. In Fig. 5, gray-level maps of OFC and EOFC departures for expansion motion are presented, where darker points represent higher values of departures.

By observing Table II, it can be noted that in the case of pure rotation around the X- and Y-axes (i.e., $\Omega_1 \neq 0$ and $\Omega_2 \neq 0$), the EOFC is better than OFC for modeling the velocity field (the ratio of 1/4 can be observed). In addition, in this case, the OFC and EOFC departures are presented as gray-level maps
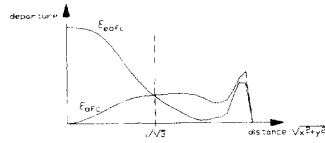
Fig. 4. Behavior of the departures of the OFC and EOFC in modeling the velocity field as a function of the distance from the image center (pure expansion motion with $l = 10$ units, isotropic illumination, noncalibrated optical system).
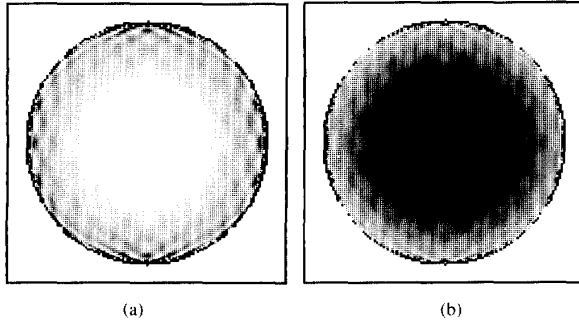

(a)   (b)

Fig. 5. Maps of the departures of (a) OFC and (b) EOFC in modeling the velocity field (pure expansion motion with $l = 50$ units, isotropic illumination, noncalibrated optical system).
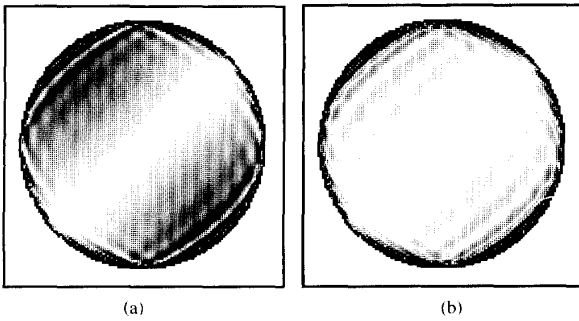

(a)   (b)

Fig. 6. Maps of the departures of (a) OFC and (b) EOFC in modeling the velocity field (pure rotational motion around X- and Y-axes, isotropic illumination, noncalibrated optical system).

(see Fig. 6). By observing these maps, it can be noted that the distribution of the departures in the 2-D plane is in accordance with the expressions of the departures as derived in Section IV.

Table III shows the departures of the OFC and EOFC in modeling the velocity field in the case of a calibrated optical system estimated in the same conditions of Table II. It can be noted that the OFC model performs better than the EOFC in all motion conditions in accordance with results derived in Section III.

In Tables IV and V, mean errors in estimating the velocity field by using OFC and EOFC are presented for both cases of calibrated and noncalibrated optical systems. Mean errors are evaluated according to $\bar{\eta}_\perp = 1/M \sum_i^M \frac{|\mathcal{E}|}{\|\nabla E\|}$, where M defines the area covered by the projection of the sphere disregarding boundaries, and $\mathcal{E}$ is the departure of the OFC or EOFC in modeling the velocity field. Although ∇E has a nonuniform distribution on the image plane, it can be

TABLE III
DEPARTURES OF OFC AND EOFC IN MODELING THE VELOCITY FIELD (MEAN VALUES AND VARIANCES) (ISOTROPIC ILLUMINATION, CALIBRATED OPTICAL SYSTEM)

isotropic illumination - calibrated optical system				
Motion	$\mathcal{E}_{ofc}$	$\mathcal{E}_{eofc}$	$Var(\mathcal{E}_{ofc})$	$Var(\mathcal{E}_{eofc})$
Translational $(W_3 = 0)$	0.092	0.092	0.009	0.009
Rotational around Z-axis	0.044	0.044	0.004	0.004
Parallel to the image plane	0.034	0.034	0.002	0.002
Expansion	0.024	3.012	0.001	0.054
Rotational around X-and Y-axes	0.056	0.320	0.029	0.122

TABLE IV
ERRORS IN THE ESTIMATION OF VELOCITY FIELD BY MEANS OF THE OFC AND EOFC (MEAN VALUES AND VARIANCES) (ISOTROPIC ILLUMINATION, NONCALIBRATED OPTICAL SYSTEM)

isotropic illumination - non-calibrated optical system				
Motion	$\bar{\eta}_{ofc\perp}$	$\bar{\eta}_{eofc\perp}$	$Var(\eta_{ofc\perp})$	$Var(\eta_{eofc\perp})$
Translational $(W_3 = 0)$	0.0781	0.0781	0.0082	0.0082
Rotational around Z-axis	0.0055	0.0055	0.0001	0.0001
Parallel to the image plane	0.0401	0.0401	0.0023	0.0023
Expansion	0.0677	0.4844	0.1525	0.6418
Rotational around X- and Y-axes	0.0697	0.0179	0.0087	0.0005

TABLE V
ERRORS IN THE ESTIMATION OF VELOCITY FIELD BY MEANS OF THE OFC AND EOFC (MEAN VALUES AND VARIANCES) (ISOTROPIC ILLUMINATION, CALIBRATED OPTICAL SYSTEM)

isotropic illumination - calibrated optical system				
Motion	$\bar{\eta}_{ofc\perp}$	$\bar{\eta}_{eofc\perp}$	$Var(\eta_{ofc\perp})$	$Var(\eta_{eofc\perp})$
Translational $(W_3 = 0)$	0.0120	0.0120	0.0001	0.0001
Rotational around Z-axis	0.0055	0.0055	0.0001	0.0001
Parallel to the image plane	0.0044	0.0044	0.0001	0.0001
Expansion	0.0033	0.5278	0.0001	0.3757
Rotational around X- and Y-axes	0.0070	0.0528	0.0001	0.0082

TABLE VI
DEPARTURES OF OFC AND EOFC IN MODELING THE VELOCITY FIELD (MEAN VALUES AND VARIANCES) (UNIFORM ILLUMINATION, NONCALIBRATED OPTICAL SYSTEM)

uniform illumination - non-calibrated optical system				
Motion	$\mathcal{E}_{ofc}$	$\mathcal{E}_{eofc}$	$Var(\mathcal{E}_{ofc})$	$Var(\mathcal{E}_{eofc})$
Translational $(W_3 = 0)$	0.349	0.349	0.043	0.043
Rotational around Z-axis	0.028	0.028	0.001	0.001
Parallel to the image plane	0.176	0.176	0.009	0.009
Expansion	0.301	2.158	0.017	0.414
Rotational around X- and Y-axes	0.165	0.073	0.011	0.006

noted that the relationships between the departures are also conserved for the estimation errors of the velocity field. Therefore, in the case of a calibrated optical system, the OFC is a better model than the EOFC for estimating the velocity field (see Table V).

B. Uniform Light Source

In Table VI, the mean values of the departures of the OFC and EOFC are reported when the optical system is noncalibrated. In addition, in this case, results agree with conclusions as derived in Sections III and IV.

Comparing Tables II and VI, it can be noted that the departures estimated in the case of a uniform illumination are always smaller that those estimated in the case of an isotropic illumination. This is due to that fact that under a uniform illumination, the image irradiance is reduced by a factor that depends on the scalar product $\mathbf{N}_s(\mathbf{P}) \cdot \mathbf{N}_c$, which is always less than 1. This reduction reflects on the departure values since these directly depend on the image irradiance.

Table VII shows the departures of the OFC and EOFC in modeling the velocity field estimated in the same conditions as Table VI, except that in this case, the camera has been

TABLE VII
DEPARTURES OF OFC AND EOFC IN MODELING THE
VELOCITY FIELD (MEAN VALUES AND VARIANCES)
(UNIFORM ILLUMINATION, CALIBRATED OPTICAL SYSTEM)

uniform illumination - calibrated optical system				
Motion	$\mathcal{E}_{ofc}$	$\mathcal{E}_{eofc}$	$Var(\mathcal{E}_{ofc})$	$Var(\mathcal{E}_{eofc})$
Translational ($W_3 = 0$)	0.045	0.045	0.003	0.003
Rotational around Z-axis	0.035	0.035	0.002	0.002
Parallel to the image plane	0.028	0.028	0.001	0.001
Expansion	0.019	2.662	0.001	0.167
Rotational around X-and Y-axes	0.176	0.447	0.019	0.080

TABLE VIII
ERRORS IN THE ESTIMATION OF VELOCITY FIELD BY MEANS OF
THE OFC AND EOFC (MEAN VALUES AND VARIANCES)
(UNIFORM ILLUMINATION, NONCALIBRATED OPTICAL SYSTEM)

uniform illumination - non-calibrated optical system				
Motion	$\eta_{ofc\perp}$	$\eta_{eofc\perp}$	$Var(\eta_{ofc\perp})$	$Var(\eta_{eofc\perp})$
Translational ($W_3 = 0$)	0.0769	0.0769	0.0095	0.0095
Rotational around Z-axis	0.0055	0.0055	0.0001	0.0001
Parallel to the image plane	0.0412	0.0412	0.0041	0.0041
Expansion	0.0659	0.4570	0.0073	0.1929
Rotational around X- and Y-axes	0.0371	0.0185	0.0034	0.0012

TABLE IX
ERRORS IN THE ESTIMATION OF VELOCITY FIELD BY MEANS OF
THE OFC AND EOFC (MEAN VALUES AND VARIANCES)
(UNIFORM ILLUMINATION, CALIBRATED OPTICAL SYSTEM)

uniform illumination - calibrated optical system				
Motion	$\eta_{ofc\perp}$	$\eta_{eofc\perp}$	$Var(\eta_{ofc\perp})$	$Var(\eta_{eofc\perp})$
Translational ($W_3 = 0$)	0.0124	0.0124	0.0002	0.0002
Rotational around Z-axis	0.0055	0.0055	0.0001	0.0001
Parallel to the image plane	0.0045	0.0045	0.0001	0.0001
Expansion	0.0032	0.5393	0.0001	0.5452
Rotational around X and Y-axes	0.0351	0.0880	0.0035	0.0167

calibrated. In addition, in this case, the OFC model performs better than the EOFC in all motion conditions.

In Tables VIII and IX, errors in estimating the velocity field by using OFC and EOFC are presented for both calibrated and noncalibrated optical systems. The considerations derived in the case of isotropic illumination for the relationships between the estimation errors of velocity field still hold in this case. Therefore, in these conditions as well, the OFC is a better model than the EOFC for estimating the velocity field

VI. CONCLUSION

Conditions have been analyzed under which different optical flow constraint equations model the velocity field. Analytical expressions of departures of distinct constraints in modeling the velocity field have been derived for different motion conditions under different types of illumination for both cases of calibration and noncalibration of the optical system. Experimental evidence has been reported, showing the mean errors induced by these departures in the estimation of the velocity field. Results show that in the presence of noncalibrated optical systems, the EOFC is a better model than the OFC for estimating the velocity field for rotational motion around the X- and Y-axes and for expansion motion in the outer parts of the image, as opposed to OFC. This is due to the fact that the EOFC compensates, to some extent, the absence of calibration in the optical system. In the presence of a calibrated optical system, the OFC model is preferable to the EOFC to estimate the velocity field for all motion conditions. The same conclusions apply to both cases of isotropic and uniform illuminations.

APPENDIX A

In this appendix, the total derivative of the image brightness is evaluated under the assumptions of an isotropic light source, Lambertian surfaces, and locally rigid patterns. In these conditions, the image irradiance has the form reported in (15). Therefore, its total derivative is

$$\frac{dE}{dt} = \frac{d\rho(\mathbf{p}, t)}{dt} \frac{\pi}{4} \left(\frac{D}{l}\right)^2 \frac{(\mathbf{P} \cdot \hat{\mathbf{Z}})^4}{(\mathbf{P} \cdot \mathbf{P})^2}$$
$$+ \rho(\mathbf{p}, t) \frac{d}{dt} \left(\frac{\pi}{4} \left(\frac{D}{l}\right)^2 \frac{(\mathbf{P} \cdot \hat{\mathbf{Z}})^4}{(\mathbf{P} \cdot \mathbf{P})^2}\right).$$

$$\frac{dE}{dt} = \frac{d\rho(\mathbf{p}, t)}{dt} \frac{\pi}{4} \left(\frac{D}{l}\right)^2 \frac{(\mathbf{P} \cdot \hat{\mathbf{Z}})^4}{(\mathbf{P} \cdot \mathbf{P})^2}$$
$$+ \rho(\mathbf{p}, t) \frac{\pi}{4} \left(\frac{D}{l}\right)^2 \frac{dB}{dt}$$

where

$$B = \frac{(\mathbf{P} \cdot \hat{\mathbf{Z}})^4}{(\mathbf{P} \cdot \mathbf{P})^2},$$

and

$$\frac{dB}{dt} = 4 \frac{(\mathbf{P} \cdot \hat{\mathbf{Z}})^4}{(\mathbf{P} \cdot \mathbf{P})^2} \left(\frac{\dot{\mathbf{P}} \cdot \hat{\mathbf{Z}}}{Z} - \frac{\mathbf{P} \cdot \dot{\mathbf{P}}}{\mathbf{P} \cdot \mathbf{P}}\right).$$

Since the patterns in the scene are supposed to be locally rigid (i.e., $\frac{d\rho(\mathbf{p},t)}{dt} = 0$), the obtained expression for dE/dt is equal to (17).

APPENDIX B

In this appendix, the total derivative of the image brightness is evaluated under the assumptions of uniform light source, Lambertian surfaces, and locally rigid patterns. In these conditions, the image irradiance has the form reported in (22). Therefore, its total derivative is

$$\frac{dE}{dt} = \frac{d\rho(\mathbf{p}, t)}{dt} (\mathbf{N}_s(\mathbf{P}) \cdot \mathbf{N}_e) \frac{\pi}{4} \left(\frac{D}{l}\right)^2 \frac{(\mathbf{P} \cdot \hat{\mathbf{Z}})^4}{(\mathbf{P} \cdot \mathbf{P})^2}$$
$$+ \rho(\mathbf{p}, t)(\mathbf{N}_s(\mathbf{P}) \cdot \mathbf{N}_e) \frac{\pi}{4} \left(\frac{D}{l}\right)^2 \frac{dB}{dt}$$
$$+ \rho(\mathbf{p}, t) \frac{\pi}{4} \left(\frac{D}{l}\right)^2 \frac{(\mathbf{P} \cdot \hat{\mathbf{Z}})^4}{(\mathbf{P} \cdot \mathbf{P})^2} \frac{d(\mathbf{N}_s(\mathbf{P}) \cdot \mathbf{N}_e)}{dt}. \quad (40)$$

Taking into account the results obtained in Appendix A, since $\frac{d\rho(\mathbf{p},t)}{dt} = 0$, the expression for dE/dt is

$$\frac{dE}{dt} = 4E \left(\frac{\dot{\mathbf{P}} \cdot \hat{\mathbf{Z}}}{Z} - \frac{\mathbf{P} \cdot \dot{\mathbf{P}}}{\mathbf{P} \cdot \mathbf{P}}\right) + \rho(\mathbf{p}, t) \frac{\pi}{4} \left(\frac{D}{l}\right)^2$$
$$\frac{(\mathbf{P} \cdot \hat{\mathbf{Z}})^4}{(\mathbf{P} \cdot \mathbf{P})^2} (\mathbf{N}_e \cdot \mathbf{\Omega} \times \mathbf{N}_s(\mathbf{P})).$$

REFERENCES

[1] B. K. P. Horn and B. G. Schunck, "Determining optical flow," *Artif. Intell.*, vol. 17, pp. 185–203, 1981.
[2] H.-H. Nagel, "Displacement vectors derived from second-order intensity variations in image sequences," *Comput. Vision. Graphics. Image Processing*, vol. 21, pp. 85–117, 1983.
[3] R. M. Haralick and J. S. Lee, "The facet approach to optical flow," in *Proc. Image Understanding Workshop (Sci. Applications)*, Arlington, VA (L. S. Baumann, Ed.), 1983.
[4] O. Tretiak and L. Pastor, "Velocity estimation from image sequences with second order differential operators," in *Proc. 7th IEEE Int. Conf. Patt. Recogn.*, 1984, pp. 16–19.
[5] A. Verri, F. Girosi, and V. Torre, "Differential techniques for optical flow," *J. Opt. Soc. Amer. A*, vol. 7, pp. 912–922, May 1990.
[6] P. Nesi, A. DelBimbo, and J. L. C. Sanz, "Multiconstraints-based optical flow estimation and segmentation," in *Proc. Int. Workshop Comput. Architecture Machine Perception*, Paris, Dec. 1991, pp. 419–426.
[7] J. P. H. van Santen and G. Sperling, "Elaborated reichardt detectors," *J. Opt. Soc. Amer. A*, vol. 2, pp. 300–321, Feb. 1985.
[8] E. H. Adelson and J. R. Bergen, "Spatiotemporal energy models for the perception of motion," *J. Opt. Soc. Amer. A*, vol. 2, pp. 284–299, Feb. 1985.
[9] D. Heeger, "Model for the extraction of image flow," *J. Opt. Soc. Amer. A*, vol. 4, pp. 1455–1471, Aug. 1987.
[10] L. Jacobson and H. Wechsler, "Derivation of optical flow using a spatiotemporal-frequency approach," *Comput. Vision, Graphics. Image Processing*, vol. 38, pp. 29–65, 1987.
[11] L. S. Davis, Z. Wu and H. Sun, "Contour-based motion estimation." *Comput. Vision, Graphics. Image Processing*, vol. 23, pp. 313–326, 1983.
[12] J. H. Duncan and T. Chou, "Temporal edges: The detection of motion and the computation of optical flow," in *Proc. 2nd IEEE Int. Conf. Comput. Vision ICCV '88*, Tampa, FL 1988.
[13] H.-H. Nagel, "On a constraint equation for the estimation of displacement rates in image sequences," *IEEE Trans. Patt. Anal. Machine Intell.*, vol. 11, pp. 13–30, Jan. 1989.
[14] A. Verri and T. Poggio, "Motion field and optical flow: Qualitative properties," *IEEE Trans. Patt. Anal. Machine Intell.*, vol. 11, pp. 490–498, May 1989.
[15] B. G. Schunck, "The motion constraint equation for optical flow," in *Proc. 7th IEEE Int. Conf. Pattern Recogn.*, 1984. pp. 20–22.
[16] ———, "Image flow: Fundamentals and future research," in *Proc. IEEE Conf. Comput. Vision Patt. Recogn., CVPR '85*, San Francisco, CA, June 19–23 1985, pp. 560–571.
[17] ———, "Image flow continuity equations for motion and density," in *Proc. Workshop Motion: Representation Anal.* Charleston, SC, May 7–9, 1986, pp. 89–94.
[18] P. Nesi, "Variational approach for optical flow estimation managing discontinuities," *Image Vision Comput.*, vol. 11, no. 7, pp. 419–439, 1993.
[19] B. G. Schunck, "The image flow constraint equation," *Comput. Vision, Graphics, Image Processing*, vol. 35, pp. 20–46, 1986.
[20] A. DelBimbo, P. Nesi, and J. L. C. Sanz, "Optical flow estimation by using classical and extended constraints," in *Proc. 4th Int. Workshop Time-Varying Image Processing Moving Object Recogn.*, June 10–11, 1993.
[21] ———, "Innovative multipoint solutions for optical flow estimation with different constraints," in *Proc. Int. Conf. Image Anal. Processing, IAPR*, Bari, Italy, Sept. 20–23, 1993.
[22] D. Willick and Y.-H. Yang, "Experimental evaluation of motion constraint equations," *CVGIP: Image Understanding*, vol. 54, pp. 206–214, Sept. 1991.
[23] C. Longuet-Higgins and K. Prazdny, "The interpretation of a moving retinal image," *Proc. Roy. Soc. London B*, vol. 208, pp. 385–397, 1980.
[24] M. Born and E. Wolf, *Principle of Optics.* New York: Pergamon, 1959.
[25] B. K. P. Horn, *Robot Vision.* Cambridge, MA: MIT Press, 1986.
[26] B. K. P. Horn and R. W. Sjoberg, "Calculating the reflectance map," *Applied Opt.*, vol. 18, no. 11, pp. 1770–1779, 1979.
[27] M. Bertero, T. A. Poggio and V. Torre, "Ill-posed problems in early vision," *Proc. IEEE*, vol. 76, pp. 869–889, Aug. 1988.
[28] B. G. Schunck, "Image flow: Fundamental and algorithms," in *Motion Understanding. Robot and Human Vision* (W. N. Martin and J. K. Aggarwal, Eds.). Boston: Kluwer, 1988, pp. 23–80.
[29] ———, "Image flow segmentation and estimation by constraints line and clustering," *IEEE Trans. Patt. Anal. Machine Intell.*, vol. 11, pp. 1010–1027, Oct. 1989.
[30] G. K. Batchelor, *An Introduction to Fluid Mechanics.* New York: Cambridge Univ. Press, 1967.

Alberto Del Bimbo (M'90) was born in Florence, Italy, in 1952. He received the doctoral degree in electronic engineering from the Faculty of Engineering of the Università di Firenze, Italy, in 1977.

He was with IBM Italia Spa during 1978–1988. Since 1988, he has been Associate Professor of Digital Systems with the Dipartimento di Sistemi e Informatica at the Università di Firenze. He has also been a reviewer for the Commission of the European Community (CEC) at the Directorate of Telecommunications, Information Industries and Innovation, Office and Business System Division. Since 1994, he has been a Full Professor of Computer Systems. His research interests and activities have been in the fields of distributed systems and image processing and presently address imaging technology, including motion analysis, pattern matching, image retrieval from databases, and visual languages.

Dr. Del Bimbo is a member of the International Association for Pattern Recognition (IAPR). Since 1991, he has been on the board of the International Technical Committee for Industrial Applications of the IAPR.

Paolo Nesi (M'92) was born in Florence, Italy, in 1959. He received the doctoral degree in electronic engineering from the University of Florence, Italy. In 1992, he received the Ph.D. degree in electronic and informatics engineering from the University of Padoa, Italy.

In 1991, he was a visitor at the IBM Almaden Research Center, San Jose, CA USA. Since November 1991, he has been with the Department of Systems and Informatics at the University of Florence, Italy, as a Researcher and Assistant Professor of both Computer Science and Software Engineering. Since 1987, he has been involved in different research topics, including motion analysis, machine vision, physical models, parallel architectures, formal languages, and real-time systems.

Dr. Nesi is a member of the International Association for Pattern Recognition (IAPR) and AIIA.
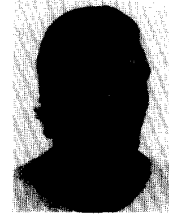
Jorge L. C. Sanz (M'82–SM'86) was born in Buenos Aires, Argentina, in 1955. He received the Master Degree in computer science in 1977 and in mathematics in 1978, both from the University of Buenos Aires. In 1981, he received the Ph.D. degree in applied mathematics, working on complexity of algorithms, from the same University.

His areas of broad professional interest are computer science and applied mathematics. Specifically, he is interested in multidimensional signal and image processing, image analysis and machine vision, parallel processing, numerical analysis, computer architectures, and other subjects. He was with the University of Buenos Aires as an instructor during 1978–1980. He was a Visiting Scientist at the Coordinated Science Laboratory, University of Illinois at Urbana-Champaign, during 1981–1982, and was an Assistant Professor there in 1983. He has been with the Computer Science Department in IBM Almaden Research Laboratory. San Jose, CA, USA, during the 1984–1994. He was the Technical Manager of the Machine Vision Group during 1985–1986. Since 1985, he has also been an Adjunct Associate professor with the University of California at Davis. He is presently Full Professor of Computer Science at the Coordinated Science Laboratory, University of Illinois, Urbana-Champaign, USA.

Dr. Sanz is an Editor-in-Chief of *Machine Vision and Applications, An International Journal* (New York: Springer Verlag). He is an author of the book *Random and Projection Transform-Based Computer Vision* (New York: Springer-Verlag, 1988). He is the editor of the book *Advances in Machine Vision* (New York: Springer-Verlag). In 1986, he received the IEEE Acoustics, Speech, and Signal Processing Society's Paper Award. He is a commitee member of the Multidimensional Signal Processing Society. He was an Associate Editor of the IEEE TRANSACTIONS ON ACOUSTICS, SPEECH, AND SIGNAL PROCESSING. He was the Guest Editor of the IEEE TRANSACTIONS ON PATTERN ANALYSIS AND MACHINE INTELLIGENCE 1988 special issues on Industrial Machine Vision and Computer Vision Technology. He has been Chair and organizer of several conferences and corkshops. He is an active member of ACM.